IMPACT OF CONCAVE AND CONVEX SOLID SURFACES BY LIQUID-LIKE PROJECTILES

Ass.Prof. Dr. Riyah N.K Ass.Prof.Dr. Sabah A.L.S
University of Anbar

ABSTRACT

A theoretical and experimental investigation of the normal impact of a flat-ended liquid slug onto ductile cylindrical solid targets is presented. The liquid slug is simulated by wax which is known to behave as a liquid in high speed impact situations. Both concave and convex types of the cylindrical target were used. The pattern of damage of the impacted Aluminum targets reveals compressed and ripple-damaged surfaces. While the convex target can be treated well by the modified model put by Kiter & Salem[5], the same cannot be said to the concave target.

KEYWORDS

Impact, concave, convex, wax, projectile.

NOTATIONS

(C_L) Speed of elastic wave in the liquid .

(C_S) Speed of elastic wave in the solid .

(C_{0L}) Speed of acoustic wave in the liquid .

(C_{0S}) Speed of acoustic wave in the solid .

(k) Physical constant of the liquid (dimensionless).

(M_0) Impact Mach number .

(P) Impact pressure .

(p) Nondimensional pressure of impact .

(q) Compression coefficient of the liquid .

(R) Radius of spherical liquid drop .

(U_0) Velocity of the undisturbed liquid .

(u_0) Nondimensional velocity of the undisturbed liquid

(U_{0n}) Normal component of the velocity of the undisturbed liquid

(u_{0n}) Nondimensional normal component of the velocity of the undisturbed liquid .

(U_{0t}) Tangential component of the velocity of the undisturbed liquid

(u_{0t}) Nondimensional tangential component of the velocity of the undisturbed liquid .

(U) Velocity of the compressed liquid .

(u) Nondimensional velocity of the compressed liquid

(U_n) Normal component of the velocity of the compressed liquid

(u_n) Nondimensional normal component of the velocity of the compressed liquid

(U_t) Tangential component of the velocity of the compressed liquid

(u_t) Nondimensional tangential component of the velocity of the compressed liquid

(V_0) Velocity of impact .

(V) Particle velocity change across shock front due to impact with a rigid surface

(V_e) Velocity of elastic solid required to give a particle velocity change (V) across shock front

(v_e) Nondimensional velocity of elastic solid required to give a particle velocity change (V) across shock front

(x_0) Radius of contact circle .

(w_0) Width of contact area .

(β) Angle of collision between colliding surfaces .

(β_c) Critical angle of collision between colliding surfaces .

(Ψ) Angle of oblique shock wave front .

(ρ_L) Density of compressed liquid .

(ρ_S) Density of compressed solid .

(ρ_{0L}) Density of undisturbed liquid .

(ρ_{0S}) Density of undisturbed solid .

(μ) Compression coefficient of target material (dimensionless)

INTRODUCTION

Material damage caused by the impact of liquid slugs has long been a problem for engineers. An aircraft in flight may

encounter water droplets which vary from a few microns in diameter up to several millimeters, and the impact of these droplets on the forward-facing surfaces of the aircraft gives rise to several design and operation problems. "Aircraft Rain Research" materialized during the 1940, s first with regard to propeller erosion and later in the 1950, s when the aviation industry entered the supersonic era[1].

The collision of a liquid with a solid surface is affected by:

1. Velocity of impact: This may be subsonic, sonic or supersonic according to the velocity of impact being respectively less than, equal to, or higher than the speed of propagation of acoustic waves in the liquid.
2. Shape and geometry: The liquid may be an extruded jet or in the form of drop or cylinder impinging on, or being hit by, stationary or moving objects. The solid objects may have flat, convex or concave cylindrical or spherical leading surfaces.
3. Angle of attack: The impact may be normal or oblique. In the case of cylindrical or spherical convex or concave solid surfaces, the impact is assumed normal provided that the path of the traveling liquid slug is a straight line passing through the center of the spherical surface, or making a right angle with the axis of cylindrical surfaces.
4. Frequency of impacts: The impact may be single or multiple for a different number of impacts.

Many investigations had been dealing with the liquid-solid impact in which the solid, the liquid or both has a curved surface[2 ,3 for example].

Bowden & Field[2] considered the case of a liquid drop of radius (R) impinging normally on a flat rigid surface with a velocity (V_0), see fig.(1). They showed that when the circumference of the contact area spreads out more rapidly than do the compression waves into the drop, outward side flow is prevented. As the drop advances, the expansion of the contact area becomes progressively slower and a point is reached where flow at the periphery of contact becomes possible. They predicted the radius of contact area at which side flow commences as:

$$x_0 = R\sin\beta = R\frac{V_0}{C_{0L}} \quad \text{.....(1)}$$

Heymann[3] rewrote eq.(1) for the critical angle at which side flow occurs as:

$$\sin\beta = \frac{V_0}{C_L} = \frac{V_0}{C_{0L} + kV_0} \quad \text{.....(2)}$$

Once the limit of the initial stage has been reached , the shock wave front becomes detached and lateral outflow from the impact zone begins. The elastic energy in the compressed

liquid is gradually transformed into kinetic energy of the lateral flow. The lateral outflow velocity can be very high[3].

Heymann[3] also applied a two-dimensional approximation adopted from the analogous problem of the oblique impact of two solid plates[4] to the impact of a spherical drop onto a rigid plane surface. By this analysis, he predicted values of the critical angle (β_c) which are smaller than those predicted by eq.(2); Full description of the analysis is given in ref.[5].

Kiter& Salem[5] modified Heymann analysis to account for the elastic response of the solid upon impact with a liquid drop. They predicted values of the critical angle(β_c) which are higher than those predicted by Heymann[3]. The main accomplishment made is that it reduces the widely cited discrepancy between the theoretical and experimental findings.

The more relevant study to the present work is that of Vickers[6] who studied the impact of a hypothetically-flat-ended cylindrical water jets against convex and concave surfaces, see fig(2). By an analysis similar to the case of a curved water surface impacting a flat plane, the impact of a flat jet hitting a convex surface, fig.(2A), gives the same result for (x_0) as that given by eq.(1). For a concave solid, fig.(2B), both outward and inward radial flows were considered separately. Vickers determined the time at which the concave surface fills with liquid and gave it as:

$$t = r_S \frac{1-\cos\beta}{V_0} \quad \text{.....(3)}$$

The diameter of the entrapped liquid was then:

$$2x_0 = d + 2r_S \frac{(1-\cos\beta)V_R}{V_0} \quad \text{.....(4)}$$

Based on the jet used in his experiments having a smooth topped mushroom-shaped head, Vickers used the value ($V_R = 6V_0$).

It was believed that the techniques employed to simulate the single liquid impact are not quite successful; regarding the work of Vickers[6], the extruded liquid jet has a leading edge which was neither controllable nor similar to what they are theoretically treated to be, so that comparison between theoretical predictions and experimental confirmations of them may be hindered[7]. Thus, Kiter& Salem[7] used wax instead, because of its liquid-like behavior at high speeds of impact, the close value of acoustic impedance to that of water and the ease with which wax projectiles of controllable shape were made[7].

Presently, flat cylindrical wax projectiles are made to impact normally onto convex and concave cylindrical targets made of Aluminum plates.

Theoretical considerations

The following analysis is essentially an extension to the analysis put by Kiter& Salem[5] for the case of a spherical liquid drop impact against a flat solid surface, see Appendix.

A flat-ended cylindrical liquid mass impinging normally at velocity (V_0) against cylindrically-convex deformable solid surface of diameter (d_S) is shown in fig.(3). As the liquid mass advances, the angle of contact (β) increases, starting from zero, resulting in elastically-deforming both the liquid mass and the solid surface. When the angle of contact attains its critical value, i.e a sonic point is reached, jetting occurs. The critical value of the contact angle is determined in the same manner described in Appendix, noting that the impact velocity is given by:

$$V_0 = U_0 \tan \beta_C \qquad (5)$$

Finally, the width of contact area (w_0) representing the initial stage of compressible behavior is given by:

$$w_0 = d_S \sin \beta_C \qquad (6)$$

The normal impact of a flat-ended liquid mass onto a cylindrically-concave, elastic, deformable surface is shown in fig.(4). At the instance of first contact, the angle of contact is:

$$\beta = \sin^{-1}\frac{d}{d_S} \quad \text{.....(7)}$$

If this angle is greater than the critical angle defined in eq.(5), jetting will occur. However, the angle of contact in this case will decrease with time, i.e ($d\beta/dt<0$) which Walsh et al.[4] regarded as a case that cannot be described by their theory; they regarded the time-dependent collision as a succession of separate (non interacting) collisions between infinitesimal plane surfaces at constant (β), provided a simple criterion is met: the angle of contact must not decrease with time, i.e ($d\beta/dt\geq 0$). This condition must be imposed to ensure non-interaction of successive members of infinitesimal collisions. In addition to this condition they stated that the proper collision at one stage of the process may be precluded by jets from an earlier stage[4]. Accordingly, the flow configuration given in fig.(4) is valid only at the first point of impact because afterwards there will be an interaction between the successive infinitesimal collisions. In addition, no initial stage of compressible behavior is possible.

EXPERIMENTAL WORK

A. Apparatus: The apparatus employed for conducting the experimental work was constructed by Kiter[8] and is used to accelerate cylindrical projectiles of wax and made to impact against cylindrical targets. This apparatus consists of many parts which are shown in fig(5).

B. Material: The material used for preparing the projectiles is Paraffin wax. A sample of this wax was analyzed and found to have the properties listed in table(1). The target material is commercially pure Aluminum supplied as a sheet plate whose thickness is (1.4mm) and having a (CLA) value of (0.32Micron). The chemical composition of this material as well as its mechanical properties are given in table(2).

C. Target holder: Concave cylindrical anvils made of hardened steel and having different diameters of (55,82,114 and 156mm) were used. For convex targets, steel drums having different diameters of (30,49,66 and 88mm) were used. In both types of tests , the concave or convex targets were aligned with the projectile by using a universal special alignment stud. Moreover, the velocity of projectile was measured by a (1953A Microsecond Fluke) counter timer aided by an electronic R-C circuit, fig.(5).

RESULTS AND DISCUSSION

A. Convex targets: Typical patterns of surface damage produced by this type of impact reveal two identical separate, symmetrical and parallel segments of eroded surface between which a rectangular region of compressed surface of the target as shown in fig.(6). Referring to fig.(3), impact occurs initially at a line which coincides with the diameter of the flat-ended projectile and is parallel to the axis of the cylindrical target as shown in fig.(6).

As impact proceeds the projectile will be subjected to compressible deformation and jetting is hindered by the attachment of the shock wave to the surface of the target as shown in fig.(3). As soon as the shock wave gets detached from the target, by the time of which the compressed region attains a critical width (w_0), jetting commences and subsequent erosion damage to the rest of the impact area is produced, as shown in fig.(6).

The width of the compressed region (w_0) was measured by using an optical measuring magnifier so that the critical angle of contact can be calculated by using eq.(6) and then correlated to the velocity of impact as shown in fig.(7). Theoretically predicted curves are also plotted in this figure for values of (k=0.7 to 1.1). It is seen that most of the experimental data lie between these curves with the curve (k=0.9) being the most suitable fit to the data. The deviation of the results at low velocities is related to the so-called (ineffective jetting) which is defined as the outward jetting which does not effect the surface damage because of its small thickness at the instant of shock wave detachment.

B. Concave targets: The pattern of the surface damage produced by the normal impact of flat-ended wax projectile onto cylindrically-concave Aluminum plates is shown in fig.(8). The figure reveals two irregular, separate segments of eroded surfaces

between which a central region of compressed surface often marked by more or less diametrical, notch-like depression.

Referring to fig.(4) and fig.(8), impact occurs initially at two points coinciding with the distal ends of the projectile diameter where the angle of contact is at its highest value. If this angle, calculated by eq.(7), is higher than the critical angle of contact, determined in eq.(5), jetting will immediately occur even at low velocities where the jetting is ineffective in eroding the surface; the jets which take the shape of a sheet, produced from both sides, meet each other, coalesce and result in the formation of two other sheet jets advancing backwards and forwards. It is the forward sheet jet which produces the notch-like diametrical depression in the surface. If the initial angle of contact in fig.(7) is equal or less than that in eq.(5), then jetting is inhibited. The critical condition can be determined by equating (β) in eq.(5) and (7). This results in:

$$d_S = d\sqrt{1+\left(\frac{U_0}{V_0}\right)^2} \qquad \text{.....(8)}$$

This theoretical prediction of the critical velocity of impact necessary to inhibit jetting were plotted for values of (k=0.7 to 1.1), see fig.(9). It can be seen that good correlation is obtained by using a value (k=1.0). Combining the estimations of the value (k) both in convex and concave targets results in an average value of (k=0.95).

Due to the fact that the angle of contact decreases with time, the critical angle of contact below which seizure of jetting is possible, will eventually be reached; in other words, the shock wave which is initially detached, will eventually be attached to the surface of the target and terminate the state of jetting. This reversed sequence of events suggests that this process of impact cannot be treated in the same way as those processes in which the angle of contact does not decrease with time. Combining the estimations of the value of (k) both in convex and concave targets results in an average value of (k=0.95).

CONCLUSIONS

The main conclusions that can be drawn from this work are:

1. The normal impact of a flat-ended wax projectile onto a cylindrically-convex rigidly-supported Aluminum plate results in eroding identical symmetrical and parallel segments of the impact area engulfing a central area of compressed surface of the target.
2. The equation of state for wax can be expressed in terms of the value (k=0.95).
3. The normal impact of a flat-ended wax projectile onto a cylindrically-concave rigidly-supported Aluminum plates also results in eroding notch-like depression of the target surface,

4. This type of impact have a reversed sequence of events to that generally encountered in time-dependent impact processes where a stage of compressible deformation is followed by jetting.

REFERENCES

1- Hwang J.B.G.; Hammitt F.G. "High-speed impact between curved liquid surfaces and rigid flat surface" Trans. ASME, J. Fluids Engng. P.396, 1977.

2- Bowden F.P.; Field J.E. "The brittle fracture of solid by liquid impact, by solid impact and by shock" Proc. Roy. Soci., V.282A, p.331, 1964.

3- Heymann F.J. "High-speed impact between a liquid drop and a solid surface" J. App. Phys., V.40, No.13, pp.5113-5122, 1969.

4- Walsh J.M.; Shreffler R.G.; Willig F.J. "Limiting conditions for jet formation in high velocity collisions" J. App. Phys., V.24, No.3, pp.349-359, 1953.

5- Kiter R.N.; Salem S.A.L. "On the elastic response of solids upon impact with a liquid drop" J. Saddam Univ.,V.6,No.2, p.136,2002.

6- Vickers G.W. "Water jet impact damage at convex, concave and flat-inclined surfaces" J. App. Mech., V.41, No.4, pp.907-911,1974.

7- Kiter R.N.; Salem S.A.L. "Simulation of the single liquid drop onto solid surfaces" J. Science and Engineering, No.2, V.2, 2002.
8- Kiter R.N. "An investigation into liquid-solid impact phenomena" Ph.D thesis, University of Baghdad, 1998.
9- Heymann F.J. "On the shock wave velocity and impact pressure in high speed liquid-solid impact" J. Basic Engng., V.90, pp.400-402, 1968.
10- Feynmann; Metropolis; Teller; Phys. Rev., 75, 1561, 1949.

APPENDIX

On the elastic response of solids upon impact with a liquid drop[5]

Since Heymann[3] restricted his analysis to the case of a liquid drop impact with a rigid surface, then an extension which includes the elasticity of the target would be of high value. The extension is made by intruding the elastic response of the target to the liquid drop impact through the momentum relations :

$$P = \rho_{0S} C_S (V_e - V) \quad \ldots\ldots(A1i)$$

And:

$$P = \rho_{0L} C_L V \quad \ldots\ldots(A1ii)$$

Because these pressures should be equal, then :

$$V_e = V\left(1+\frac{\rho_{0L}C_L}{\rho_{0S}C_S}\right) \quad \ldots\ldots(A2)$$

The continuity relation across the shock front implies that:

$$\rho_{0L}U_{0n} = \rho_L U_n \quad \ldots\ldots(A3)$$

Adopting the value of the speed of elastic wave in the liquid due to Heymann[9] ,i.e :

$$C_L = C_{0L} + kV \quad \ldots\ldots(A4)$$

The angle of contact can be evaluated as :

$$\beta = \tan^{-1}\frac{u_{0n}}{u_{0t}} - \tan^{-1}\frac{u_{0n}-v_e}{u_{0t}} \quad \ldots\ldots(A5)$$

In addition to this extension, an exact value of (C_S) is obtained by using the equation of state for the solid material compiled by Feynmann et al.[10] which is given by:

$$P = \frac{a\mu + b\mu^2 + c\mu^3 + d\mu^4 + e\mu^5}{1+1.5\mu^2} \quad \ldots\ldots(A6)$$

Where (a, b, c, d, e) are constants for a given material.

Knowing that :

$$C_S^{\,2} = \frac{1}{\rho_{0S}} \frac{dP}{d\mu} \qquad \ldots\ldots(A7)$$

The value of (C_S) can be determined as follows: for a given impact pressure (P) there is a corresponding value of (μ), given by eq.(A6), so that (C_S) can be determined by using eq.((A7) together with the first differential of (P) deduced from eq.(A6).

Full and extensive description of the analysis is given in ref.[5].

Table(1): Properties of Paraffin wax analyzed by Daura Refinery.

Density (gm/cm^3)	Melting point(^0C)	Oil content weight%	Penetration at 25^0C	Elastic wave speed (m/s)
0.825	64	1.1	23	1520

Table(2A): The chemical composition of the commercially pure Aluminum plate.

Cu	Mg	Si	Fe	Mn	Ti	Al
0.003	0.014	0.056	0.328	0.003	0.016	Remainder

Table(2B): The mechanical properties of the plate material.

Temper	Tensile strength (N/mm^2)	Elongation %	Vickers Hardness
Hard	157	2.5	41

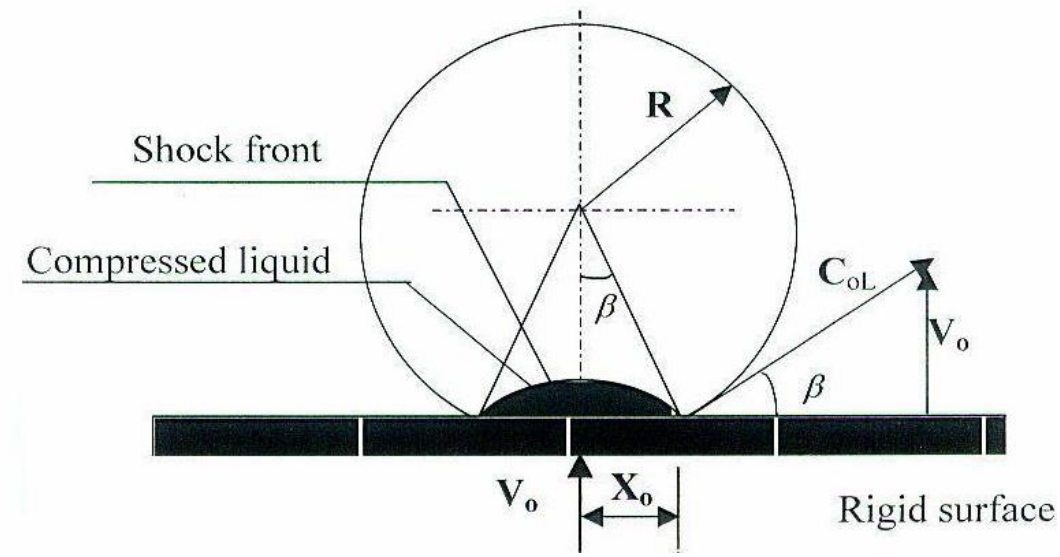

Fig.(1): Geometrical scheme of the impact of a plane against a spherical drop[2].

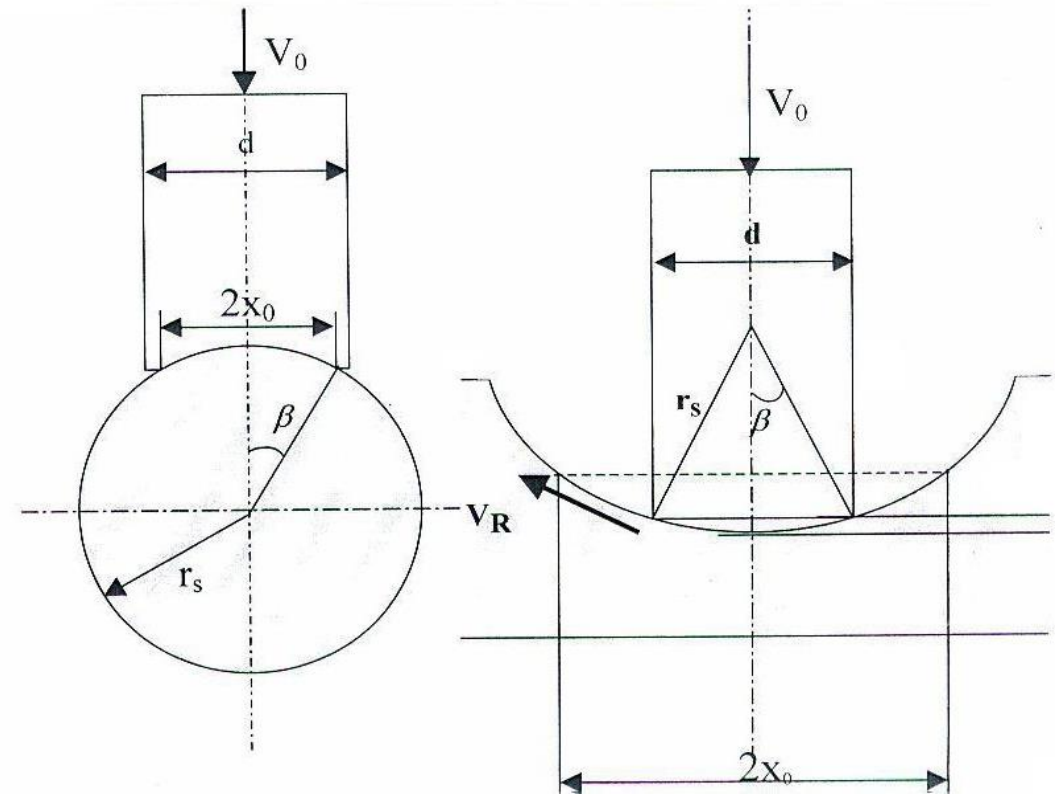

(A) (B)

Fig.(2): Schematic diagram of a liquid jet impact on: (A)Convex surface (B)Concave surface[6].

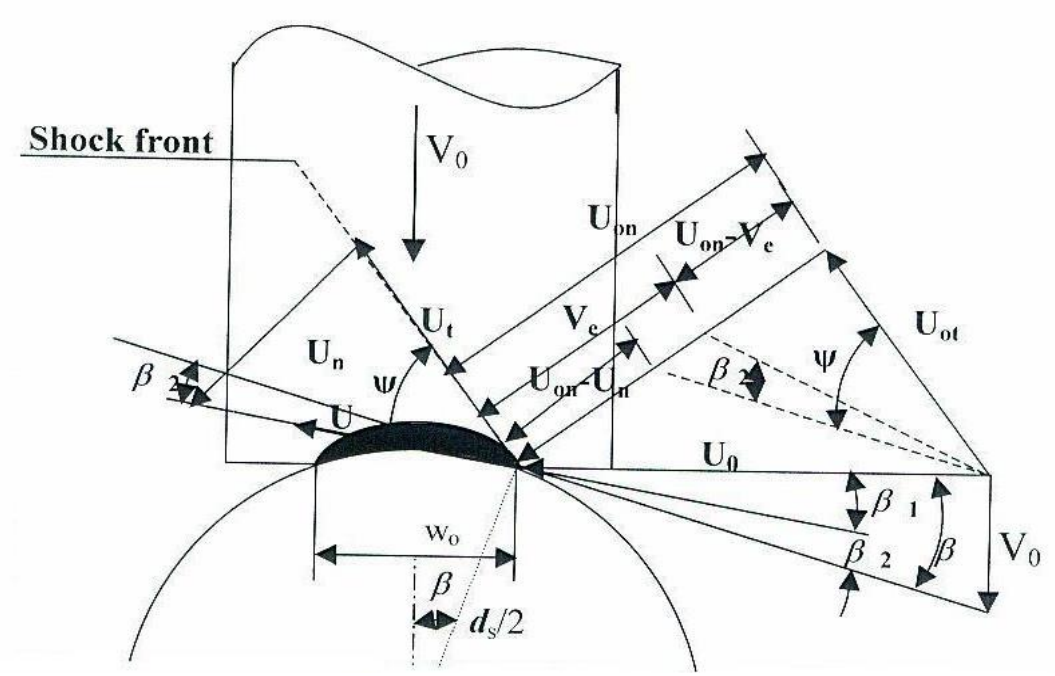

Fig.(3): Conditions at contact perimeter of a flat-ended cylindrical liquid mass impacting against a cylindrically-convex elastic solid.

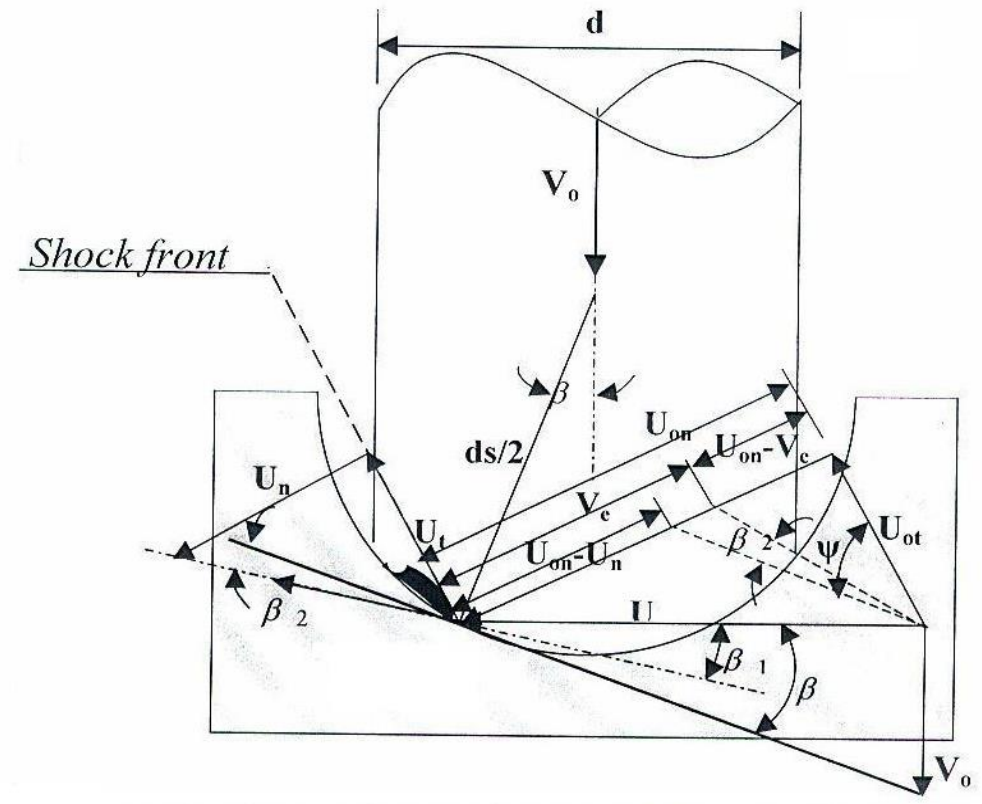

Fig.(4): Unsteady flow configuration at contact edges of flat-ended liquid impacting against a cylindrically-concave elastic solid

Fig.(5): A schematic diagram of the apparatus (shown exploded):
1. The firing mechanism 2. The cartridge 3. The cartridge holder 4. The gun barrel 5. The gun barrel support 6. The frame 7. The target holder 8. Concave target

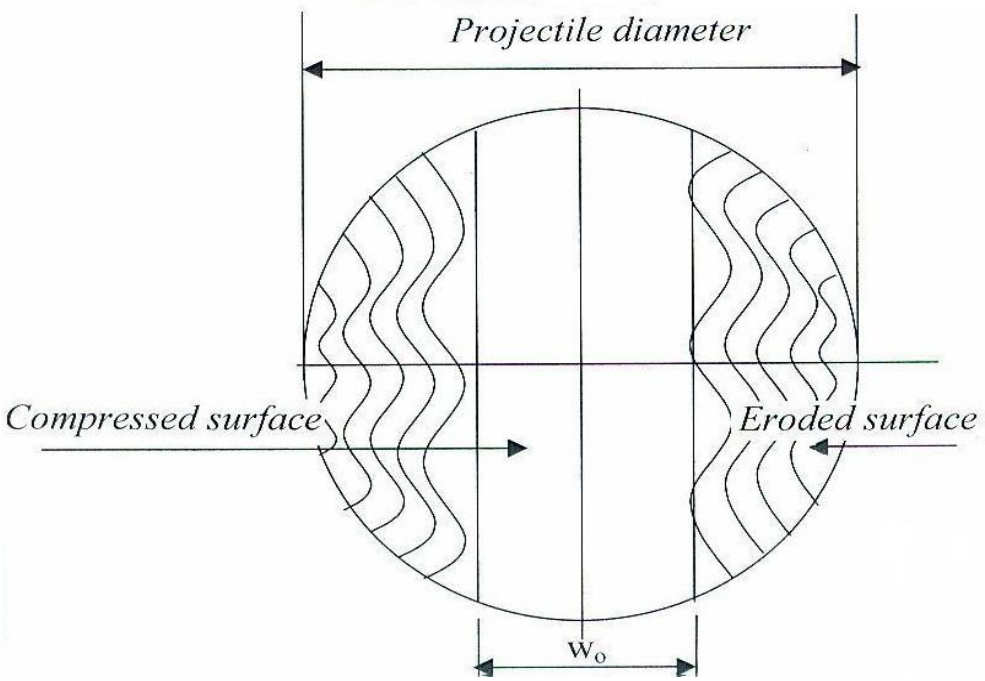

Fig.(6): Schematic of a photograph of damage surface of cylindrically-convex Aluminum plates produced by a flat-ended wax projectile.

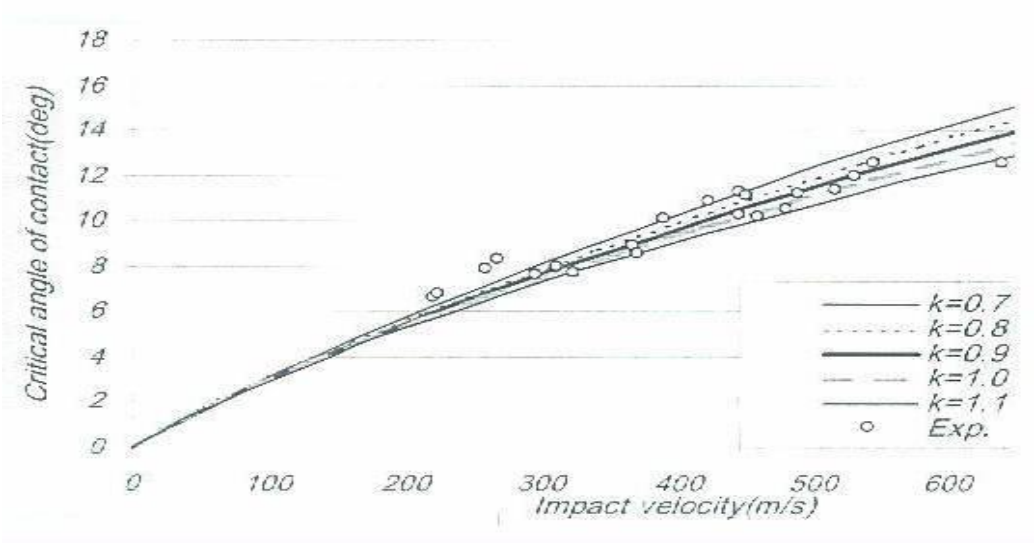

Fig.(7): Variation of measured critical angle of contact with the velocity of a flat-ended wax projectile impact onto cylindrically-convex Aluminum plates.

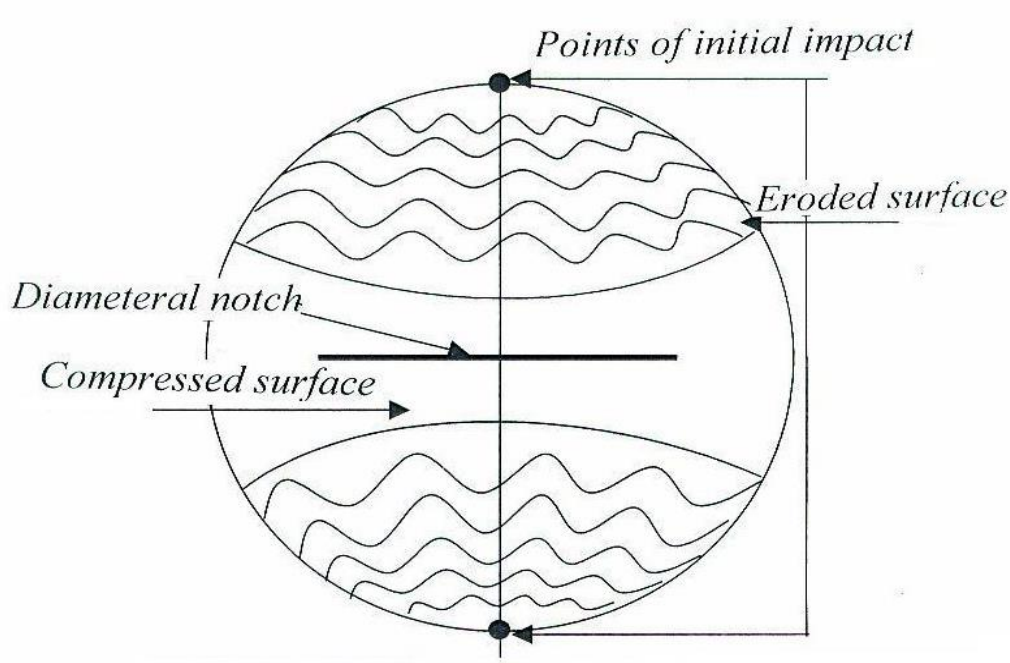

Fig.(8): Schematic of a photograph of damaged surface of cylindrically-concave Aluminum plates by flat-ended wax projectile .

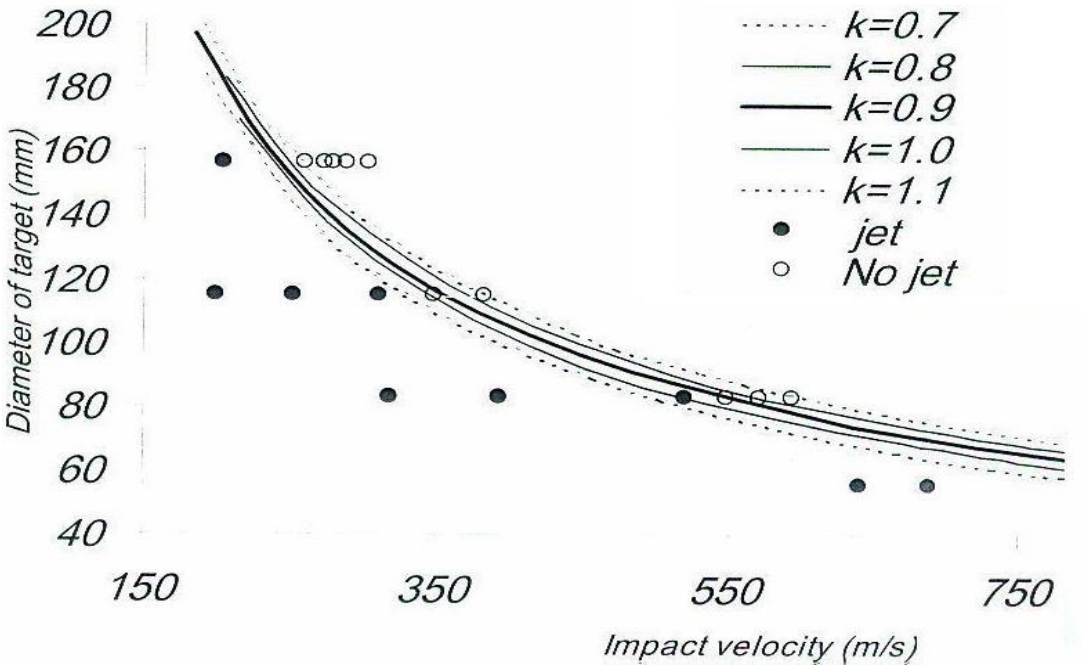

Fig.(9): Variation of the critical diameter of concave target with the velocity of a flat-ended wax projectile.

تصادم السطوح الصلبة المقعرة والمحدبة بالمقذوفات الشبيهة بالسوائل

ا.م.د . رياح نجم كطر ا.م.د .صباح عبد اللطيف

جامعة الأنبار

الخلاصة

يقدم هذا العمل بحثا"نظريا"وعمليا" للتصادم العمودي بين كتلة سائلة مستوية مع سطح اسطواني مصنوع من مادة مطاوعة . تم تمثيل الكتلة السائلة باستخدام الشمع المعروف بتصرفه الشبيه بالسوائل في حالات التصادم السريع. استخدم في البحث نوعين من الأهداف الاسطوانية المحدبة والمقعرة. أظهرت مناطق التصادم سطحين احدهما مضغوط والآخر متعري ومتموج. أمكن تطبيق موديل معدل أعد من قبل

Kiter&Salem[5] على الأهداف المحدبة بينما لا يمكن القول نفسه بشان الأهداف المقعرة.

الكلمات الدالة

تصادم، مقعر، محدب، شمع، مقذوفه.